REVISTA MATÉRIA
V.24 N.01
ISSN 1517-7076 artigo e-12322, 2019

Study of the structural and morphological properties of copper catalysts supported on Al_2O_3 and TiO_2 synthesized by the impregnation method

Germana Arruda de Queiroz [1], Celmy Maria Menezes de Bezerra Barbosa [1]

[1] Laboratório de processos catalíticos – LPC, DEQ/UFPE, CEP: 50670-901, Recife, Pernambuco, Brasil.
e-mail: germana_aqueiroz@yahoo.com.br, celmy@ufpe.br

ABSTRACT

Aluminum oxide and titanium oxide are widely used as catalytic support. Due to their characteristics and properties, they have several applications such as chemical processes, photocatalysis and pollution control. In this work, the catalytic supports of Al_2O_3 and TiO_2 were impregnated with 2% of copper oxide by the method of impregnation. The catalysts were characterized by X-ray Diffraction (XRD), Scanning Electron Microscopy (SEM), Brunauer–Emmett–Telle (BET) surface area and Infrared Spectroscopy techniques (FTIR). The results of XRD analysis presented the Cu/TiO_2 catalyst with high degree of crystallinity where the peaks corresponding to the phases anatase, rutile and CuO are easily found, while the Cu/Al_2O_3 catalyst presented low degree of crystallinity. The samples morphology is in the form of agglomeration, the specific surface area was higher when copper metal was impregnated to the supports and the highest values was obtained with Cu/Al_2O_3 catalyst. FTIR analysis allowed the visualization of the main vibrations of the functional groups presents in the catalysts samples. According to the results, it was observed that the incorporation of copper oxide did not affect significantly the crystalline structure of TiO_2 and Al_2O_3 and that at the calcination temperature of 500°C it is possible to obtain a high specific surface area and a more active phase resulting in a good characterization which is suitable for various industrial applications.

Keywords: Catalyst, Titanium, Aluminium, Hydrogen, Impregnation.

1. INTRODUCTION

Modern societies have great scientific and technological challenges for the development of new energy generation processes, preferably with the use of fuels from renewable sources, in a sustainable way, that contribute to the preservation of the environment [1]. Hydrogen, source of renewable energy, a regenerative, inexhaustible and environmentally friendly fuel with high calorific value, has attracted much attention of scientists [2,3]. It can be generated by various chemical processes, and the choice of fuel in fuel cell technology is an important factor and should be considered in its development [1,4].

Researches in the area of heterogeneous catalysis has grown in recent years due to the need to obtain clean chemically process and with low cost. The great challenge is to develop technologies that allow the substitution of polluting sources for clean and renewable sources [4]. In the case of hydrogen production, it is necessary that the catalysts have characteristics as high thermal stability, high activity and having a long service life, under the operating conditions of the system [2,5] .

The precious metals such as platinum (Pt), ruthenium (Ru), palladium (Pd) and rhodium (Rh) perform well in chemical reactions to hydrogen production [6,7]. However, due to the high cost of these metals, its production is unviable on a commercial scale, and these metals are being replaced by catalysts that use non-noble metals. Replacing noble metals by lower cost transition elements as cobalt (Co), cerium (Ce), copper (Cu), manganese (Mn) and chromium (Cr) is considered a technological advance in the catalysis area [8–10]. Copper oxide-based catalysts have been widely studied in the last 35 years due to their high activity and selectivity in processes such as methanol synthesis, water gas shift reaction, selective catalytic reduction of NOx, oxidative methanol steam reforming (SRM) as well as photocatalysis [11–13]. Among the materials studied for the catalytic support, γ-Al_2O_3 [14], silica [15] and TiO_2 [16], are promising materials and are being increasingly used as catalytic supports for the several applications.

In many publications, it has been reported that TiO_2 containing Cu particles are efficient photocatalysts for H_2 evolution [17]. The γ-alumina (γ-Al_2O_3) containing Cu also is efficient and very used as supports

Autor Responsável: Germana Arruda de Queiroz Data de envio: 16/07/2017 Data de aceite: 29/11/2017

10.1590/S1517-707620190001.0605

at industrial applications due their high specific areas. However, the improvement of copper-based catalytic system is highly required [18, 19, 24]. Therefore, due to the technological importance of catalysts to hydrogen production for the generation of energy, the aim of this work is to determine aspects and properties textural, morphologic and structural of the Cu/Al_2O_3 and Cu/TiO_2 catalysts with the following analyses XRD, SEM, BET and FTIR. The variables of processing as the calcination temperature and the method of preparation of catalyst also were analysed.

2. MATERIALS AND METHODS

2.1 Materials

The Cu catalysts (2wt% Cu/TiO_2 and 2wt% Cu/Al_2O_3) were prepared using the following reagents with the incipient impregnation method. The Titanium dioxide P25 was supplied by Evonik, formerly Degussa (Recife – PE, Brazil), the precursor salt $Cu(NO_3)_2{\cdot}3H_2O$ was supplied by Vetec Fine Chemicals and alumina by Oxiteno.

2.2 Catalyst preparation

The precursor salt, $Cu(NO_3)_2{\cdot}3H_2O$, was dissolved in distilled water in a 250-mL flask. After this dissolution, the support (TiO_2 or Al_2O_3) was added to the copper nitrate solution and it was placed in a 500-mL flask. The impregnation process occurred under continuous stirring, at 25°C for 48 hrs. After, was dried in an oven at 60 °C for 24 hrs. Posteriorly, the catalyst was taken to calcination in a fixed bed reactor heated at 500°C for 5 hours in an inert atmosphere (argon or nitrogen). The inert gas flow rate was kept at approximately 100 mL · min^{-1} during the process. After the calcination process, the catalyst was reduced with H_2 at 400 °C, using 25 mL min^{-1} flows of H_2 and N_2, for 4 hrs. The figure 1 show all scheme of impregnation process with the Cu/Al_2O_3 and Cu/TiO_2 catalysts.

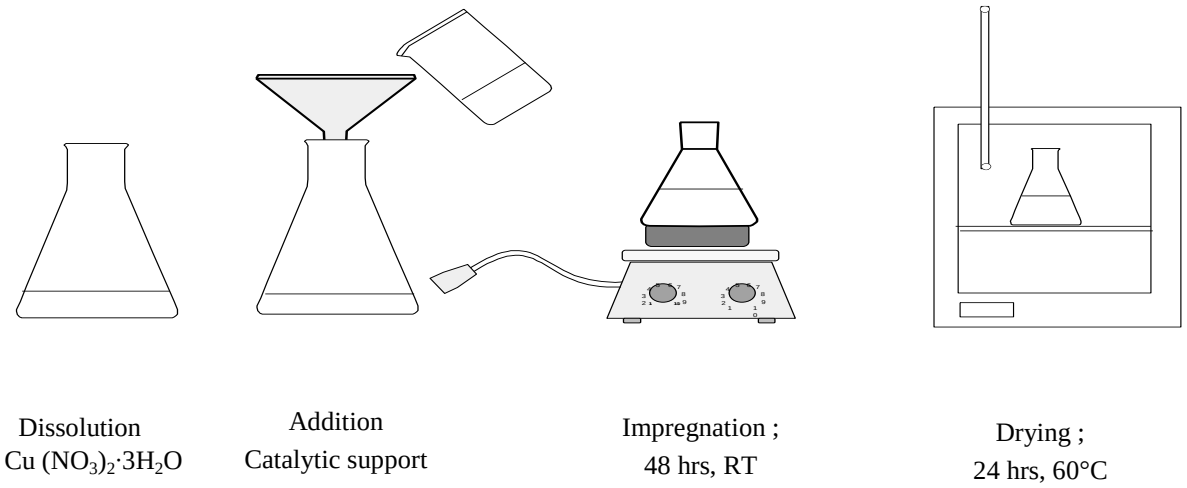

Figure 1: Scheme impregnation process for the preparation of Cu/Al_2O_3 and Cu/TiO_2 catalysts.

2.3 Characterization

The BET (BELSORPII / BEL) method was used to analyse the structural and textural characteristics, DRX (XRD-6000 Shimadzu Equipment) analysed the solid phases, SEM/EDX (SEM, FEI brand, Quanta 200 FEG, 200-30 kV) showed the morphology, and FTIR (FTIR Bruker VERTEX 70 FT-IR) identified the surface chemical groups. The samples used after the final reduction procedure.

3. RESULTS

3.1 Adsorption and desorption of N_2

The orders of magnitude superficial specific area, pore volume, and average pore size of the catalyst Cu/TiO_2 and Cu/Al_2O_3 measured by nitrogen adsorption at 77 K are shown in Table 1. In general, the catalysts are prepared with broad surface areas, as an indication of better dispersion of the active phase.

Table 1: Surface area, pore volume, and pore size of Cu/TiO_2 and Cu/Al_2O_3 catalysts.

SAMPLE	BET SURFACE AREA ($m^2.g^{-1}$)	PORE VOLUME ($Cm^3.g^{-1}$)	PORE SIZE (A)
TiO_2	75	0,14	184,2
Cu/TiO_2	61,28	0,34	183,26
Al_2O_3	208	0,69	89,33
Cu/Al_2O_3	193,32	0,45	91,81

It was observed that after the reduction process of the catalysts the support undergoes variations in the surface areas and in the volume of pores. The two catalysts decrease BET surface area after the calcination and reduction process of the catalyst at the temperature of 500 and 400 °C, respectively. It is important to note that catalysts with a high surface area value are very important, since it has possibly more active sites per mass of material, this was visualized on the alumina carrier [20]. As expected there were no major changes in pore size values.

3.2 X-ray diffraction

Figure 2a and 2b shows the diffractograms of the Cu/TiO_2 and Cu/Al_2O_3 catalysts. The crystalline phases were identified by comparison with Joint Committee on Powder Diffraction Standards (JCPDS). Figure 2a shows the XRD patterns of the CuO/TiO_2 catalyst, it was found the presence of anatase and rutile and the monoclinic crystal structure of CuO. The main TiO_2 peaks are observed at $2\theta = 25.31°$, 37.67°, and 47.95°, and peaks corresponding the rutile phase are observed at $2\theta = 27.48°$, 36.10°, and 56.57°, in all the diffractograms was attributed to the support structure of TiO_2 (JCPDS 84-1286 and JCPDS 88-1175), respectively. The peaks observed at $2\Theta = 35°$ and 38° are characteristic of copper oxide (CuO) with a monoclinic cubic crystalline system (JCPDS 080-1916). Figure 2b shows the XDR patterns of the Cu/Al_2O_3 catalyst, the diffraction peaks are observed at $2\Theta = 37$, 46 and 66º and are attributed to reflections for aluminium oxide (Al_2O_3), with crystalline cubic system (JCPDS 074-2206). The CuO copper phase was observed at $2\Theta =$ 35.6° and 61° that correspond, respectively, to the reflections (110) and (-113) with monoclinic cubic crystalline system (JCPDS 080-1916). By X-ray diffraction it is also possible to characterize metallic particles, provided they are well crystallized, with dimensions between 3 and 50 nm. The particle size can be calculated by the Scherrer equation.

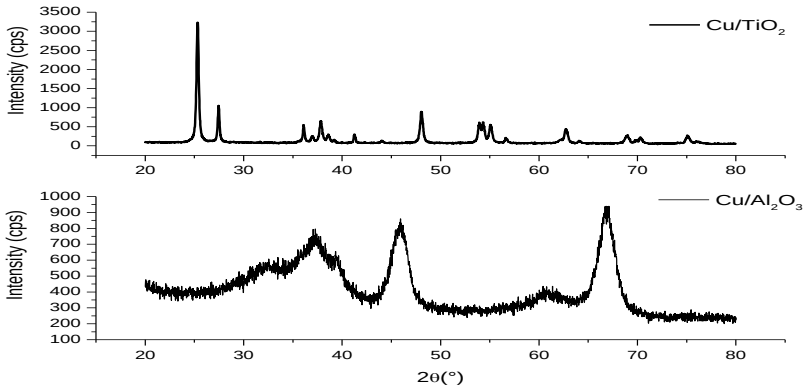

Figure 2: XRD patterns of Cu catalysts supported (a) TiO_2 and (b) on Al_2O_3.

3.3 SEM analysis

The structural morphologies of Cu/TiO_2 and Cu/Al_2O_3 are show in figure 3 (a - b) and were examined using the SEM analysis. Figures 3 (a) for the Cu/TiO_2 catalyst and 3 (b) for the Cu/Al_2O_3 catalyst. It was possible to show the morphology of supports TiO_2 and Al_2O_3. In general, the images show randomly distributed particles with varying geometries in different sizes along agglomerates in the form of irregular morphology plates for both samples. It was possible to identify the elements present in the catalytic system, being verified the presence of the substrate and metal. The elements present in Cu/Al_2O_3 were C, O, Cu, Al and in Cu/TiO_2 catalysts were C, O, Ti, Cu and can be visualized in supplementary materials.

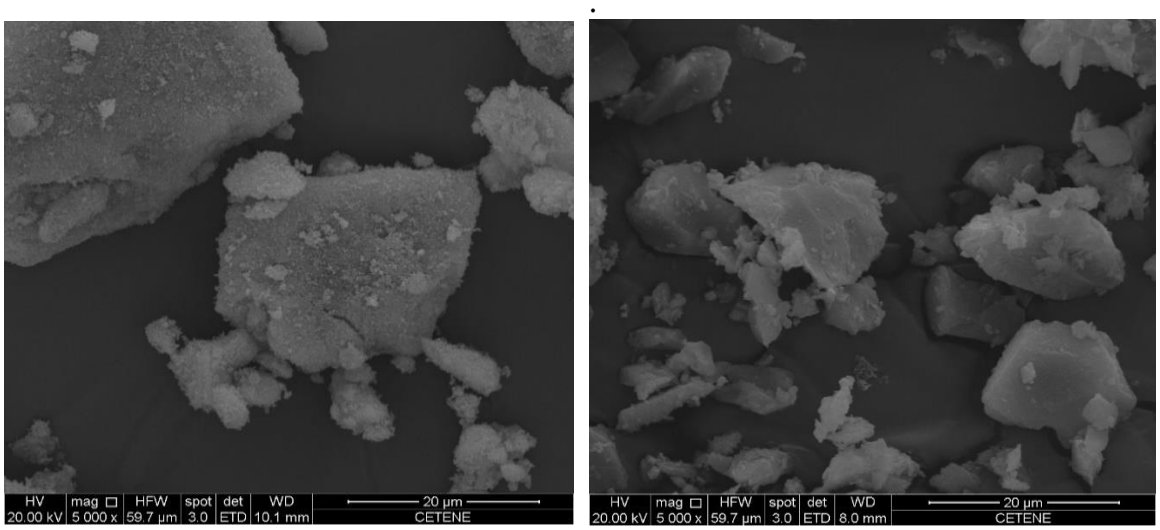

Figure 3: SEM image of (a) Cu/TiO_2 catalyst (b) Cu/Al_2O_3 catalyst.

3.4 FTIR spectrum

The FTIR spectrum of Cu/Al_2O_3 and Cu/TiO_2 catalyst in the wavelength region 4000 – 500 cm^{-1}can be visualized in figure 4 (a-b). For the Cu/Al_2O_3 catalyst, were observed the absorption bands at 3385, 1635, 1504, 1380, 838, 738 cm^{-1}. The bands at 3385 cm^{-1} and 1635 cm^{-1} were attributed to O–H bending, which can be due to physically adsorbed water [21]. The vibrations of hydroxyl groups comprise the O-H stretch derived from two contributions: (1) non-dissociated O-H species and (2) O-H species (dissociated from H_2O), both adsorbed [22,23]. The broadband range of 1500 to 700 cm^{-1} comprises two types of bonds, Al-O-H and Al-O bonds. The 1300 cm^{-1} region is related to the OH group present on the surface, and the region below 1000 cm^{-1} is characterized by metal-oxygen bonds [23]. For the Cu/TiO_2 catalyst, were observed the absorption bands at 3439, 3369, 3300, 1652, 737 and 676 cm^{-1}. The peaks at 3439 – 3300 cm^{-1} and 1652 cm^{-1} were attributed to O-H bending, and the bands observed from 400 – 900 cm^{-1} corresponded to Ti–O Anatase stretching vibrations [23].

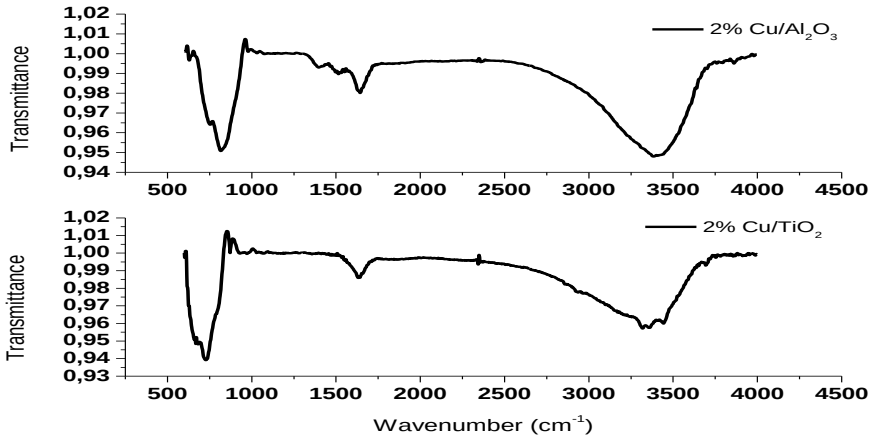

Figure 4: IR spectrum of Cu/Al_2O_3 and Cu/TiO_2 catalysts.

4. DISCUSSION

4.1 Specific surface area of Cu/TiO_2 and Cu/Al_2O_3 catalysts

The addition of the Cu to the catalytic supports Al_2O_3 and TiO_2 generated a decrease in the BET surface area, this reduction is due a blockage of the metal deposited in stricter pores or possible agglomeration of the metal on the surface, which would lead to a decrease of the area [24]. According to the IUPAC (International Union of Pure and Applied Chemistry) classification, the isotherms of adsorption / desorption of the reduced material was classified as type IV, which are characteristic of mesoporous materials with regular cylindrical and/or polyhedral pores ($2nm < \phi_{Porous} \leq 50nm$). The hysteresis was observed (figure 5) indicating that there was condensation of nitrogen at intermediate and high values of P/Po, indicating the existence of a population of pores of smaller diameter side to the larger [25, 26]. The pore size of Cu/Al_2O_3 and Cu/TiO_2 catalysts has not changed much in relation to pure support (Al_2O_3 and TiO_2), this means that the impregnation method has only little effect on the surface area of the catalyst [27]. Wang et al. [28] worked with synthesis of Titanium oxide (TiO_2) and showed that the calcination temperature cause alterations in the structure of the materials, resulting in the decrease in the enlargement of the diffraction peaks and increase of the particle size as well as a reduction of the surface area. Yu et *al*. [29] also performed the analysis of the calcination temperature for Cu/TiO_2 catalyst verifying changes in the characteristics of the material as well as in different behaviours for application in the catalysis area. Thyssen et al. [24] worked with Cu/Al_2O_3 catalysts and the analysis of the calcination temperature reduced of the surface area. Oliveira et al. [30] worked with Cu/Al_2O_3 and found BET surface are and pore volume similar to the values found in this study.

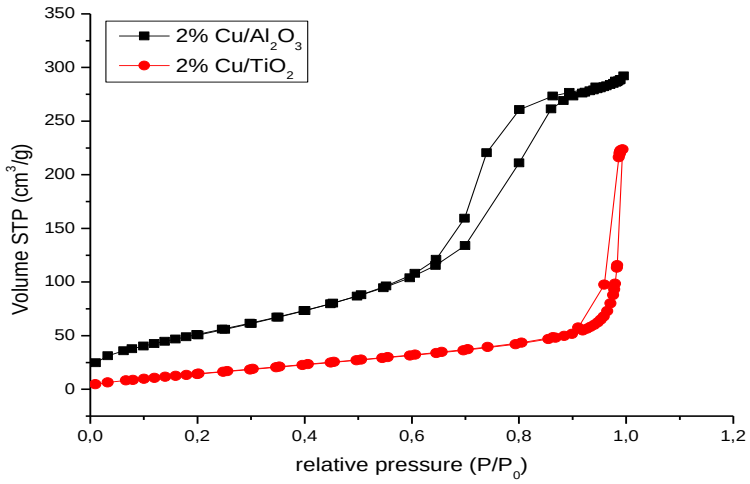

Figure 5: Adsorption and desorption isotherm of the Cu/Al_2O_3 and Cu/TiO_2 catalysts.

4.2 Structural characterization of Cu/TiO_2 and Cu/Al_2O_3 catalysts

X-ray diffraction analysis was possible to visualize the crystalline phases of copper, titanium and alumina through the X-ray diffractograms (Figure 2). In the Cu/TiO_2 catalyst, the diffraction peak of copper oxide phase observed is small due to the low amount of copper oxide present in the sample. The samples become very similar to that of the P25 TiO_2 sample. The crystallite size for anatase and rutile phase and alumina were determined by a Scherrer equation as shown in Equation 1, using the most intense peak of anatase around 2θ of 25.3°, rutile around 2θ of 27.4° and alumina around 2θ of 45°.

$$D = \frac{k.\lambda}{\beta.\cos\theta} \tag{1}$$

where D is the main crystal size of the catalyst, λ is the X-ray wavelength (1.54056 A°), β is the full width at half maximum (FWHM) of the catalyst, θ is the diffraction angle, and *k* is a shape factor, that varies from 0.89 for spherical to 0.94 for cubic particles, usually 0.90 for particles of unknown shape.

The crystal size influences the surface area of the catalyst, this knowledge is very important to surface reactions, the large crystal size may allow direct contact between the metal oxide and the catalytic support,

giving good catalyst stability, favouring catalytic performance. The average crystal size of copper oxide, aluminium and titanium has been determined. The results show crystallites with dimensions of the order of 6 to 30 nanometers of oxide copper and aluminium and 10 to 40 nanometers of oxide copper and titanium.

The catalysts were calcinated at 500°C, in general, the crystallization of TiO_2 takes place at temperatures greater than 400 ° C. Silva et al [31] worked with TiO_2 and obtained similar results. Yanan liu et al [32] showed that calcination temperature plays a dominant role in the degree of crystallinity. On the existing peaks in the sample of Cu/TiO_2, can be reported that these are narrow and of high intensity, which indicates the high crystallinity of TiO_2 support. The anatase crystalline phase is predominant due to a greater amount and intensity of its peaks. In the Cu/Al_2O_3 catalyst, the peaks were low crystallinity. In the literature reports that calcinated aluminium oxide at temperatures up to 650 °C, has low crystallinity with wide peaks and high porosity. Additionally, the structures of the materials were preserved when compared to the XRD of the pure supports reported by Zhu et *al*. [33] for TiO_2, by Park et *al*. [34] for γ-Al_2O_3.

Figure 4 shows the FTIR results for samples of the Cu/TiO_2 and Cu/Al_2O_3 catalysts. For the Cu/TiO_2 catalyst, the broad bands around 3800 - 2500 cm^{-1} and 1620 - 1651 cm^{-1} correspond to the stretching vibrations of O-H and bending vibrations of strongly adsorbed water molecules coordinated to Ti^{4+} in the catalysts, respectively [21,28]. This result means that even calcined at 500°C for 6 h, the samples still retain large amount of OH groups. The main peak at 400–900 cm^{-1} was attributed to Ti-O stretching and Ti-O-Ti bridging stretching modes [21]. The Cu/Al_2O_3 catalyst presented the same characteristics in relation to the broad bands corresponding to the vibrations of O-H, because they were prepared with the same method. It is important to point out that the existence of this type of bonding on the surface of the material, since they exert a great effect in the coordination of the atoms in the surface, leading to different properties and energetic states. This in turn directly affects the stability of the crystalline form, since the existence depends on the energy balance between surface and volume of the material.

4.3 Morphological analysis of Cu/TiO_2 and Cu/Al_2O_3 catalysts

The calcination process also affects the morphologies of the catalysts, as shown in Figure 3, the micrographs of the Cu/TiO_2 and Cu/Al_2O_3 catalysts obtained by SEM. After calcination treatment, the samples are composed of randomly distributed particles with different sized geometries adjacent to agglomerates in the form of plates. For the Cu/TiO_2 catalyst, this may be caused by the phase transformation from anatase to rutile, resulting in the decrease in the pore volume (as shown in Table 1). The method of impregnation also influenced in the morphologic of the samples. Wang et al [28] worked with TiO_2 and showed that the calcination process affect the morphology of the samples, after calcination treatment the samples are composed of larger agglomerated particles. Rana et al [23] synthesized $Cu_{2.6}$–$Zn_{0.5}/TiO_2$ catalyst at different magnifications. The rough spherical morphology and slight agglomeration can be seen on the structure of catalyst, the slight agglomeration present on the surface might be due to the sintering during the calcination process. For the Cu/Al_2O_3 catalyst, the alumina can be obtained with different morphological and textural properties, depend on the synthesis of the precursor hydroxide and thermal treatment of transformation of this hydroxide into transition alumina. There was no sphericity of the alumina particles in the samples analysed.

5. CONCLUSION

In this work, the BET surface area was of 193,32 $m^2 . g^{-1}$ and 61,28 $m^2 . g^{-1}$ to Cu/Al_2O_3 and Cu/TiO_2 catalyst, respectively. The addition of copper particles on the support of alumina and titanium decreased the surface area value. Copper particles were detected in the XDR analysis, but could not be visualized in the microscopy analysis. The crystal size was calculated and a particle size in the range of 10-30 nanometers for the Cu/Al_2O_3 catalyst and in the range of 10-40 nanometers for the Cu/TiO_2 catalyst was obtained. In the FTIR functional groups were identified. From these results can conclude that from a simple route for the method of synthesis and using low-cost CuO particles we can be obtained a good material that it can be directed to specific applications such as hydrogen production, obtained from chemical processes or in photocatalysis.

6. ACKNOWLEDGMENTS

Federal University of Pernambuco - UFPE, PRH 28 - Petroleum Human Resources, Ministry of Science and Technology, FINEP - Innovation and Research, and CETENE – Northeast Technology Center.

7. BIBLIOGRAPHY

[1] BERGAMASCHI, V.S., *Preparação e Caracterização de Catalisadores de metais de transição suportados em Zircônia uso na reforma a vapor do etanol para obtenção de hidrogênio*, Tese de D.Sc., Universidade de São Paulo, SP, Brasil, 2005.

[2] NEEF H.J., "International overview of hydrogen and fuel cell research", *Energy*. v.34, n.3, pp.327–33, 2009.

[3] WANG, H.Z., LEUNG, D.Y.C., LEUNG, M.K.H., *et al*., "A review on hydrogen production using aluminum and aluminum alloys", *Renewable & Sustainable Energy Reviews*, v.13, n.4, pp.845–53, 2009.

[4] BALZER R. *Síntese e caracterização de catalisadores óxidos metálicos para oxidação catalítica total de btx (benzeno, tolueno e orto-xileno) e transformação química de monoterpenos*, Tese de D.Sc., Universidade Federal de Santa Catarina, SC, Brasil, 2014.

[5] JOHNSTON B., "Hydrogen: the energy source for the 21st century", *Technovation*, v.25, pp.569–585, 2005.

[6] SMITH, R. J. B., LOGANATHAN, M., SHANTHA, M.S. "A Review of the Water Gas Shift Reaction Kinetics", *International Journal Chemical Reactor Engineering*, v.8, n.1, pp. 1–32, 2010.

[7] RATNASAMY, C., WAGNER, J.P., "Water Gas Shift Catalysis", Catalysis Reviews: Science and Engineering v.51, n.3, pp. 325–440, 2009.

[8] DELACOURT, C., NEWMAN J. "Mathematical modeling of CO2 reduction to CO in aqueous electrolytes: II. Study of an electrolysis cell making syngas (CO+H2) from CO2 and H2O reduction at room temperature", *Journal of the Electrochemical Society*, v.157, n.12, pp. 1911–26, 2010.

[9] LEBEDEVA, N. P., ROSCA, V., JANSSEN G.J.M. "CO oxidation and CO2 reduction on carbon supported PtWO3 catalyst", *Electrochimica Acta*, v.55, n.26, pp.7659–68, 2010.

[10] ZHAN, Z. L., ZHAO L. "Electrochemical reduction of CO2 in solid oxide electrolysis cells", *Journal Power Sources*, v. 195, n.21, pp.7250–7254, 2010.

[11] PIRES, C.A., SANTOS, A.C.C., JORDAO, E. "Oxidation of phenol in aqueous solutions with copper oxide catalysts supported on γ-Al2O3, Pillared Clay and TiO2: comparison of the performance and costs associated with each catalyst", *Brazilian Journal Chemical Engineering*, v.32, n.4, pp.937–848, 2015.

[12] RAKOCZY, J., NIZIOŁ, J., WIECZOREK-CIUROWA, K., *et al*., "Catalytic characteristics of a copper-alumina nanocomposite formed by the mechanochemical route", *Reaction Kinetics Mechanisms Catalysis*, v.108, n.1, pp.81–9, 2013.

[13] CHEN, W.H., LIN, M.R., JIANG, T.L., *et al*., "Modeling and simulation of hydrogen generation from high-temperature and low-temperature water gas shift reactions", *International Journal Hydrogen Energy*, v. 33, n.22, pp.6644–56, 2008.

[14] MASSA, P., IVORRA, F., HAURE, P., *et al*., "Optimized wet-proofed CuO/Al2O3 catalysts for the oxidation of phenol Enhancing, Solutions: catalytic stability", *Catalysis Communications*, v.10, pp.1706–1710, 2009.

[15] NJIRIBEAKO, A. I., HUDGINS, R. R., SILVESTON P.L. "Catalytic oxidation of phenol in aqueous solution over copper oxide", *Industrial Engineering Chemical Fundamental*, v.173, pp.234–44, 1978.

[16] DÜKKANCÝ, M., GÜNDÜZ G. "Catalytic wet air oxidation of butyric acid and maleic acid solutions over noble metal catalysts prepared on TiO2", *Catalysis Communications*, v. 10, pp.913–9, 2009.

[17] JUNG, M, NG, Y.H, JIANG, Y., *et al*., "Active Cu species in Cu/TiO2 for photocatalytic hydrogen evolution", In: Chemeca 2013 (41st: 2013: Brisbane, Qld.). Chemeca 2013: Challenging Tomorrow. Barton, ACT: Engineers Australia, pp. 214-217, 2013.

[18] YANG, X, WANG, S, SUN, H, *et al*., "Preparation and photocatalytic performance of Cu-doped TiO2 nanoparticles", *Transactions of Nonferrous Metals Society of China*, v.25, n.2, pp.504–509, 2015.

[19] MOREIRA, M.N., RIBEIRO, A.M., CUNHA, A.F., *et al*., "Copper based materials for water-gas shift

equilibrium displacement", *Applied Catalysis B: Environmental*, v.189, pp. 199–209, 2016.

[20] CALDAS, P.C. P. *Estudo das propriedades estruturais dos catalisadores de Cu e Cu-Ce suportados em alumina aplicados à reação de deslocamento gás-água catalisadores de Cu e Cu-Ce suportados em gás-água*, Dissertação de M.Sc., Universidade Federal de São Carlos, São Paulo, Brasil, 2013.

[21] YU, J. G., SU, Y. R., CHENG, B., *et al*., "Effects of pH on Mesoporous, themicrostructures and photocatalytic activity of Hydrothermal, nanocrystalline titania powders prepared via Method", *Journal Molecular Catalysis A Chemical*, v. 258, pp.104–112, 2006.

[22] CARVALHO, D.C. *Estudo da Influência dos Íons Mg e Zr na Transição de Fase Amorfo-Gama da Alumina*, Dissertação de M.Sc., Escola Politecnica da Universidade de São Paulo, São Paulo, Brasil, 2012.

[23] RANA, A.G., AHMAD, W., AL-MATAR, A., *et al*., "Synthesis and characterization of Cu–Zn/TiO2 for the photocatalytic conversion of CO 2 to methane", *Environmental Technology*, v.38, n.9, pp. 1085-1092, 2016.

[24] THYSSEN, V. V., MAIA, T. A., ASSAF, E. M. "Cu and Ni Catalysts Supported on γ-Al2O3 and SiO2 Assessed in Glycerol Steam Reforming Reaction", *Journal of the Brazilian Chemical Society*, v. 26, n.1, pp.22-31, 2015.

[25] WEBB, P. A., ORR, C., "Analytical Methods in Fine Particle Technology", *Micromeritics Instruments Corp*., pp. 24, 1997.

[26] SING, K.S.W., EVERETT, D.H., HAUL, R.A.W., *et al*., "Reporting physisorption data gas/solid systems with special reference to the determination of surface area and porosity", *Pure and Applied Chemistry*, v. 57, pp.603–619, 1985.

[27] BEHNAJAD M. A., ESKANDARLOO H., "Silver and copper co-impregnated onto TiO2-P25 nanoparticles and its photocatalytic activity", *Chemical Engineering Journal*, v.228, pp.1207–1213, 2013.

[28] WANG, G., XU, L., ZHANG, J., *et al*., "Enhanced photocatalytic activity of TiO2 powders (P25) via calcination treatment", *International Journal of Photoenergy*, v. 2012, Article ID 26576, 2012.

[29] YU, J. G., YU, H. G., CHENG, B., *et al*., "Enhanced photocatalytic activity of TiO2 powder (P25) by hydrothermal treatment", *Journal Molecular Catalysis A Chemical*, v.253, n.1–2, pp.112–118, 2006.

[30] OLIVEIRA, N.M.B. *Reação de deslocamento de gás d'Água sobre catalisadores de cobre e níquel suportados em alumina e nanofibra de carbono*, Dissertação de M.Sc., Campinas, São Paulo, Brasil, 2012.

[31] SILVA, W. L., LANSARIN, M. A., MORO CC. "Síntese, Caracterização e atividade fotocatalítica de catalisadores nanoestruturados de TiO2 dopados com metais", *Quimica Nova*, v.36, n.3, pp.382–386, 2013.

[32] YANAN, LIU., HE, J.U.N., SUN, Y.U., *et al*., "A comparison of N-doped TiO2 photocatalysts preparation methods and studies on their catalytic activity", *Journal Chemical Technology Biotechnology*, v.88, n.10, pp.1815 – 1821, 2013.

[33] ZHU, J., AHANG, D., BIAN, Z., *et al*., "Aerosol-spraying synthesis of SiO2/ TiO2 nanocomposites and conversion to porous TiO2 and single-crystalline TiOF2", *Chemical Communications*, n.36, pp.5394–5396, 2009.

[34] PARK, J. W., JEANG, J. H., YOON, W. L., *et al*., "The co-promoted CuO-CeO2/γ-Al2O3 catalyst for the selective oxidation of CO in excess hydrogen", *Applied Catalysis A: General*, v. 274, pp.25–32, 2004.

ORCID

Germana Arruda de Queiroz https://orcid.org/0000-0001-9155-417X
Celmy Maria Menezes Bezerra Barbosa https://orcid.org/0000-0003-3280-0048